

Arbitrary Precoding with Single-Fed Parasitic Arrays: Closed-Form Expressions and Design Guidelines

Vlasis I. Barousis and Constantinos B. Papadias, *Fellow, IEEE*

Abstract—Single-fed compact arrays known as electronically steerable parasitic antenna radiators (ESPARs) have recently emerged as a new paradigm for spatial multiplexing that requires only a single radio-frequency (RF) chain and a few easy-to-implement analog tunable loads. Besides the remarkable hardware savings, the ESPAR capabilities are still limited as it is not possible to find appropriate loadings that multiplex *any* signaling format over the air. Indeed, commonly the loading values are obtained through time-consuming iterative algorithms, e.g. exhaustive search, and can only emulate MIMO transmission of signals emerging from low-order constellations. This paper constitutes a clear step forward in solving this problem, as it defines the necessary guidelines for the design of single-fed ESPAR systems that are able to support *an arbitrary* precoding scheme. To alleviate the need for iterative processes, the proposed design methodology uses complex tunable loads and introduces new closed-form expressions for the exact computation of the loads and the feeding voltage.

Index Terms—Parasitic antenna arrays, ESPAR, compact arrays, spatial multiplexing, space-time coding.

I. INTRODUCTION

ESPAR arrays were first proposed by Gyoda and Ohira [1], as an extension of the parasitic array introduced by Harrington in [2]. Instead of the conventional trend of arrays with multiple RF chains, ESPARs require only a single RF chain that feeds the sole active element, as shown in see Fig. 1. The active element is surrounded by multiple parasitics that are weighed with analog tunable loads. Thanks to the dense deployment of the elements and the strong coupling among them, current is induced at all parasitics. As is shown in (1), further current control is possible by tuning the analog loads:

$$\mathbf{i} = v_s(\mathbf{Z} + \mathbf{Z}_G)^{-1}\boldsymbol{\delta}_1 = v_s\mathbf{G}^{-1}\boldsymbol{\delta}_1 \quad (1)$$

where $\mathbf{Z} \in \mathbb{C}^{(N \times N)}$ is the mutual coupling matrix that depends on the ESPAR's geometry and $\mathbf{Z}_G = \text{diag}(R_s, x_2, \dots, x_N) \in \mathbb{C}^{(N \times N)}$ is the diagonal loading matrix that holds the x_m , $m = 1, 2, \dots, N - 1$ complex loading values and the output resistance of the source R_s that typically equals 50Ω . Furthermore, v_s is the complex voltage fed to the sole active element and $\boldsymbol{\delta}_1 \in \mathbb{C}^{(N \times 1)}$ is a selection vector. The remarkable size savings due to the requirement for dense deployment of elements make ESPARs a promising technology, suitable for lightweight hand-held devices or small access points with strict power and size constraints. So far, they had been proposed for low cost analog beamforming

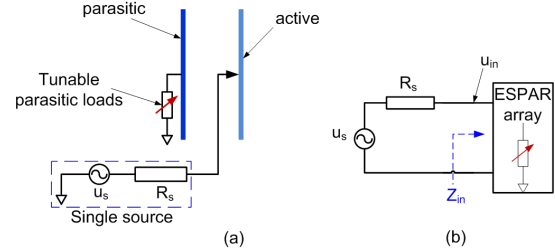


Fig. 1. ESPAR with one active and one parasitic element. The equivalent topology is also shown.

(e.g. [1]) that is achieved by tuning purely imaginary loads. The pioneering work in [3] laid the foundation for single RF MIMO transmission with ESPARs. By switching imaginary parasitic loads, the authors therein achieve spatial multiplexing of low order PSK signals over the air. Similar **heuristic load switching patterns** were adopted in other works on the topic, e.g. [4]. Given a certain ESPAR geometry (usually formed by simple dipoles), a common challenge in these early works was to estimate the parasitic loads that enable the ESPAR to multiplex signals over the air with the **highest possible modulation order**. The loads were obtained iteratively via exhaustive search methods or stochastic optimization algorithms [5], [6]. In both cases, a level of uncertainty should be accepted since the convergence to the global minimum of the cost-function and the estimation of the optimal loading values is not guaranteed a-priori. A proof-of-concept experiment in [7] validated the concept, while a detailed overview of single RF MIMO with ESPAR arrays can be found in [8].

As it is understood, the preceding work usually assumes an arbitrary ESPAR array formed by dipoles and the main effort is to obtain the sets of loading values that exploit **to the maximum the multiplexing capabilities** of the given ESPAR. On the contrary, this paper focuses on the design conditions that an ESPAR array should satisfy in order to support *an arbitrary* precoding scheme that would be desired for a certain application. Simple beamforming, or MIMO transmission of any signaling format, e.g. beyond PSK, are special cases. The rest of the paper is organized as follows: Section II provides closed-form expressions and lays out the guidelines to design ESPAR array systems that are able to support any desired transmission scheme. A complex loading with the real part ranging from negative to positive values is a key-enabler toward this goal (for a circuit design of such a load see [9]). In the same Section, a conventional ESPAR array example with two dipole elements will be assumed for demonstration purposes and better understanding of all aspects. As an application, Section III presents a new ESPAR

Manuscript received December 10, 2013. The associate editor coordinating the review of this letter and approving it for publication was K. K. Wong.

The authors are with the Broadband Wireless and Sensor Networks Group, Athens Information Technology (AIT), 19.5 km Markopoulo Avenue, 19002 Peania, Athens, Greece (e-mail: {vbar, cpap}@ait.gr).

Digital Object Identifier 10.1109/WCL.2014.020614.130863

$$\begin{bmatrix} Z_{11} + R_s & Z_{12} & \cdots & Z_{1N} \\ Z_{21} & Z_{22} + x_1 & \cdots & Z_{2N} \\ \vdots & \vdots & \ddots & \vdots \\ Z_{N1} & Z_{N2} & \cdots & Z_{NN} + x_{N-1} \end{bmatrix} \begin{bmatrix} i_0 \\ i_1 \\ \vdots \\ i_N \end{bmatrix} = \begin{bmatrix} v_s \\ 0 \\ \vdots \\ 0 \end{bmatrix} \quad (2)$$

system that has been designed according to the methodology and guidelines shown in Section II and is able to support the **Alamouti precoding scheme** with QAM signaling modulation. The key findings of the paper are summarized in Section IV.

II. ARBITRARY PRECODING WITH ESPARS

A. Loading and feeding computation

Expanding (1) we get (2), from which the complex feeding voltage and the loading values of an arbitrary ESPAR array can be easily obtained as a function of the desired port currents:

$$\begin{aligned} x_n &= -\mathbf{z}_n^{(r)} \mathbf{i} / i_n, n = 1, 2, \dots, N-1 \\ v_s &= \mathbf{g}^{(r)} \mathbf{i} \end{aligned} \quad (3)$$

where $\mathbf{z}_n^{(r)}$ is the n -th row of the coupling matrix \mathbf{Z} , i_n is the n -th port current and $\mathbf{g}^{(r)}$ is the first row of \mathbf{G} . The input impedance as seen from the single feeding port (see Fig.1) is a function of the normalized vector of currents $\mathbf{i}_{\text{nor}} = \mathbf{i}/i_0$:

$$Z_{\text{in}} = \mathbf{z}_1^{(r)} \mathbf{i}_{\text{nor}} = Z_{11} + \sum_{m=2}^N Z_{1m} \frac{i_{m-1}}{i_0} \quad (4)$$

B. ESPAR Radiation

As (4) indicates, the input impedance depends on the normalized currents, which in turn means that it is a function of the loading values¹. Therefore, an arbitrary vector of port currents might cause $\Re\{Z_{\text{in}}\} < 0$, implying a negative radiation resistance. In such a case, the ESPAR would not radiate and would instead consume power. For demonstration purposes and better understanding, in this Section the following coupling matrix is considered, as obtained from the IE3D antenna software² at $f_c = 2.6$ GHz:

$$\mathbf{Z} = \begin{bmatrix} 45.12 - j16.60 & 42.39 - j29.51 \\ 42.39 - j29.51 & 42.95 - j29.64 \end{bmatrix} \quad (5)$$

Applying for example a load³ $x = -37.23 + j9.89\Omega$ to the ESPAR in (5), an input impedance of $Z_{\text{in}} = -84.29 - j25.98\Omega$ is measured in IE3D. This result can be also validated by combining (1) and (4) for $v_s = 1$. The reflection coefficient in this case will be $S_{11} = 10$ dB, as can be computed by [10]:

$$S_{11} = 20\log_{10}(|\rho|), \quad \rho = \frac{Z_{\text{in}} - Z_s^*}{Z_{\text{in}} + Z_s} \quad (6)$$

¹It is also a function of the frequency, but here the carrier frequency is assumed.

²IE3D is a full-wave, method-of-moments based electromagnetic simulator that solves the current distribution on 3D and multilayer structures of general shape and is provided by Mentor Graphics.

³Throughout the paper, the computation of the loads and the results are independent of the load implementation. The circuit implementation itself is not within the scope of this work. There are a variety of possible circuits to generate the required loads, possibly offering different trade-offs of performance vs. complexity. An example of such a design is presented in [9], but other designs are possible as well.

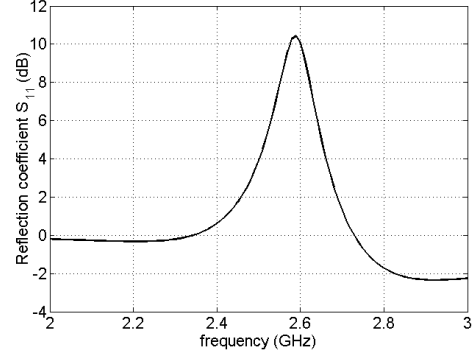


Fig. 2. Example of positive reflection coefficient due to $\Re\{Z_{\text{in}}\} < 0$.

where usually $Z_s = R_s = 50\Omega$. This result agrees with Fig.2 that is obtained from IE3D. Definitely a positive reflection coefficient indicates $\Re\{Z_{\text{in}}\} < 0$, which is not realistic as it would imply that the reflected power is higher than the incoming to the input ports. To avoid such a situation, an ESPAR design should satisfy the following condition:

Design condition: An ESPAR array is able to support an arbitrary precoding set $S = \{\mathbf{s}_1, \mathbf{s}_2, \dots, \mathbf{s}_Q\}$, $\mathbf{s}_q \in \mathbb{C}^{(N \times 1)}$ if

$$a_q > -\Re\{Z_{11}\}, \quad a_q = \Re\left\{\sum_{m=2}^N Z_{1m} \frac{i_{m-1}^{[q]}}{i_0^{[q]}}\right\}, \quad (7)$$

for all possible input currents $\mathbf{i}_q = \mathbf{s}_q, q = 1, 2, \dots, Q$.

Proof: As has been explained, an ESPAR design can support the precoding set S when for all possible input currents $\mathbf{i}_q = \mathbf{s}_q, q = 1, 2, \dots, Q$ it is $\Re\{Z_{\text{in}}^{[q]}\} > 0$. Then, taking also into account (4) we conclude directly (7). ■

In other words, the appropriate ESPAR array should be designed with large enough real part of the self impedance of the feeding element and with an appropriate inter-element spacing, so that (7) is satisfied for all combinations of port currents. Meanwhile, it is noted that a load impedance with $\Re\{Z_{\text{in}}\} < 0$ connected to a typical source forms the fundamental topology of the so-called negative resistance oscillators [11]. This implies that under certain loading configurations the topology in Fig.1 would be unstable. However, such a case has been already prevented by the constraint in (7).

C. ESPAR Matching

Equation (1) implies an unmatched situation where the feeding port of the ESPAR is connected directly to a single source with a typical output resistance of $R_s = 50\Omega$. As the input impedance of the ESPAR depends highly on the loading values, or equivalently the port currents, different loadings will cause high mismatch effects, i.e. different levels of reflection coefficients S_{11} and a shift of the resonant frequency of the

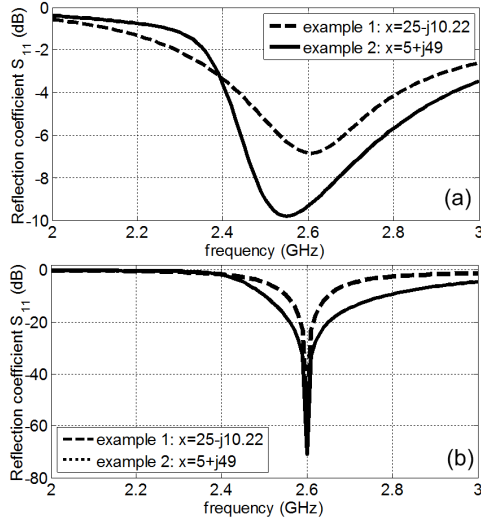


Fig. 3. Indicative reflection coefficients a) without matching and b) under perfect dynamic matching.

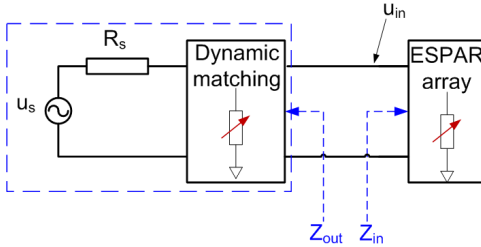


Fig. 4. ESPAR array with dynamic matching.

ESPAR. Such an example is shown in Fig.3(a) obtained from IE3D for randomly selected loading values. To account for both effects, a dynamic matching between the source and the ESPAR is required as shown in Fig.4, which is tuned along with the parasitic loading. In this case, the resonant frequency remains fixed and also the reflection coefficients are negligible. This is shown in Fig.3(b), which is an updated version of Fig.3(a). Such a dynamic matching could be realized with varactor diodes and lumped elements. In Fig.4 it can be easily shown that the output impedance of the source including the matching network is

$$Z_{out} = \hat{Z}_{22} - \frac{\hat{Z}_{12}\hat{Z}_{21}}{\hat{Z}_{11} + R_s} \quad (8)$$

where \hat{Z} is a matrix with the Z parameters of the two port network that represents the dynamic matching circuit. Under perfect matching, Z_{out} is equal to the complex conjugate of the ESPAR's input impedance at the carrier frequency, i.e.

$$Z_{out} = Z_{in}^* \quad (9)$$

To take into account the dynamic matching circuit, \mathbf{Z}_G in (1) is modified as $\mathbf{Z}_G = \text{diag}(Z_{out}, x_2, \dots, x_N)$ and (3) is used to compute the new feeding voltage.

D. Extension to Multiple Active & Parasitic Elements

Assuming an array with M active out of N elements, M feeding voltages are required, accompanied by M two-port

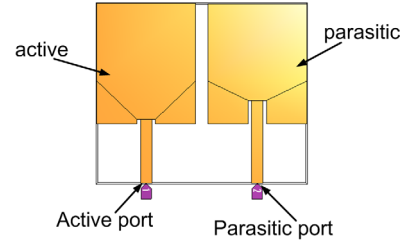


Fig. 5. Top view of a realistic ESPAR array designed in IE3D.

networks $Z_{out}^{[m]}$, $m = 1, 2, \dots, M$ that similarly to (9) match the input impedances $Z_{in}^{[m]}$, $m = 1, 2, \dots, M$ of the array as seen by the corresponding ports. In this case (2) still applies if the M loading values are replaced by $Z_{out}^{[m]}$, $m = 1, 2, \dots, M$ and the M zeros with the corresponding feeding voltages $v_s^{[m]}$, $m = 1, 2, \dots, M$. It is noted that this approach provides further flexibility but the additional RF chains will increase linearly the hardware burden.

III. APPLICATION EXAMPLE

As an indicative example, an ESPAR array is designed using the methodology and guidelines shown in Section II. We choose to implement the Alamouti space-time precoding scheme [12] with QAM signaling constellation.

A. ESPAR design

The array (see Fig.5) consists of two patch elements designed on a FR4 substrate of height 1.52mm with dielectric constant of $\epsilon_r = 3.2$ and dielectric loss tangent of $\tan\delta = 0.017$. The self impedance Z_{11} and Z_{22} is controlled mainly by the inset, which as observed is different for each patch element. The coupling matrix of this array at 2.6 GHz, as obtained from IE3D design software is

$$\mathbf{Z} = \begin{bmatrix} 465.4 - j659.5 & -24.06 + j34.93 \\ -24.06 + j34.93 & 21.12 - j157.2 \end{bmatrix} \quad (10)$$

B. ESPAR Evaluation

According to the Alamouti scheme [12], given a signal vector $[s_1 \ s_2]^T$ the port currents in (1) should be adjusted so that

$$\mathbf{i} = \underbrace{\begin{bmatrix} s_1 & -s_2^* \\ s_2 & s_1^* \end{bmatrix}}_{\text{time}} \quad (11)$$

Therefore, the port currents are equal to $[s_1 \ s_2]^T$ during the first signaling period, and equal to $[-s_2^* \ s_1^*]^T$ during the second signaling period. The loading value, the feeding voltage and the input impedance can be computed analytically for each desired current vector by (3) and (4) respectively.

The appropriate ESPAR array should meet the requirements described in (7) for all possible combinations in (11). This constraint guarantees that $\Re\{Z_{in}\} > 0, \forall i$ and therefore the ESPAR array will radiate and a matching is possible. In case of 16-QAM signaling, there are 256 possible vectors $[s_1 \ s_2]^T$, but due to (11) the ESPAR array should be able

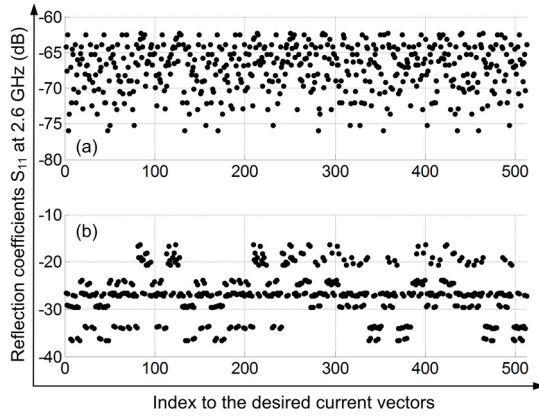


Fig. 6. Reflection coefficients in case of Alamouti scheme with 16-QAM signals, a) dynamic matching, b) fixed matching to the mean value of Z_{in} .

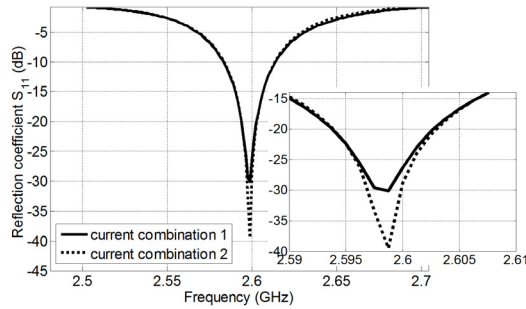


Fig. 7. Indicative reflection coefficient plots in case of Alamouti scheme with 16-QAM signals, as obtained from IE3D for the array in Fig.5.

to adjust $Q = 512$ possible combinations of port currents. Applying these current vectors to (7) we get $\min_{q=1,2,\dots,Q} (a_q) = -104.79 > -\Re\{Z_{11}\}$, which due to (7) means equivalently that $\Re\{Z_{in}\} > 0$ for all current combinations in (11). Figure 6(a) shows all reflection coefficients at the target frequency of 2.6GHz assuming a dynamic matching, i.e. $Z_{out}^n = \langle (Z_{in}^n)^* \rangle, \forall q = 1, 2, \dots, Q$ (see also (9)), where $\langle \cdot \rangle$ indicates an operator that rounds to the nearest integer. As expected, the reflection coefficient remains always below -60 dB. However, as is shown in Fig.6(b), a fixed matching circuit with $Z_{out} = (E\{Z_{in}\})^*$, where $E\{\cdot\}$ denotes the operand of the mean value, is enough as the reflection coefficients are always below -15 dB. It is mentioned that the design in Fig.5 can support up to 128-QAM signaling, but in this case a fixed matching is not enough and it should be changed dynamically along with the loading values. For completeness, Fig. 7 illustrates the reflection coefficients for the first two current combinations, as obtained from IE3D, where an L-type matching is used for convenience that does not allow for bandwidth control. To overcome this problem, a T (or its equivalent Π) type network should be used instead [13]. A wider bandwidth could be also obtained by increasing the inter-element spacing [14] and/or by selecting an appropriate

shape of the ESPAR elements [15]. The zoomed region shows a good agreement with the first two points in Fig.6(b) that are obtained theoretically at 2.6GHz as -26.56dB and -29.14dB respectively.

IV. CONCLUSION

This paper provides a new methodology and guidelines for the design of single-RF parasitic arrays that are able to support an arbitrary precoding scheme and an arbitrary signaling constellation. An indicative design example is shown that achieves space-time precoding with 16-QAM signaling. Although generally a dynamic network may be required, it has been shown that for certain precoding sets and single-RF designs, even a fixed matching network suffices.

ACKNOWLEDGMENT

This work has been supported by the EU FP7 project HARP, under grant number 318489.

REFERENCES

- [1] T. Ohira and K. Gyoda, "Electronically steerable passive array radiator antennas for low-cost analog adaptive beamforming," in *Proc. 2000 IEEE International Conference on Phased Array Systems and Technology*, pp. 101–104.
- [2] R. F. Harrington, "Reactively controlled directive arrays," *IEEE Trans. Antennas Propag.*, vol. 26, no. 3, pp. 390–395, 1978.
- [3] A. Kalis, A. G. Kanatas, and C. B. Papadimas, "A novel approach to MIMO transmission using a single RF front end," *IEEE J. Sel. Areas Commun.*, vol. 26, no. 6, pp. 972–980, 2008.
- [4] O. N. Alrabadi, C. B. Papadimas, A. Kalis, and R. Prasad, "A universal encoding scheme for MIMO transmission using a single active element for PSK modulation schemes," *IEEE Trans. Wireless Commun.*, vol. 8, no. 10, pp. 5133–5142, 2009.
- [5] C. S., A. Hirata, T. Ohira, and N. C. Karmakar, "Fast beamforming of electronically steerable parasitic array radiator antennas: theory and experiment," *IEEE Trans. Antennas Propag.*, vol. 52, no. 7, pp. 1819–1832, 2004.
- [6] V. Barousis, A. G. Kanatas, A. Kalis, and C. Papadimas, "A stochastic beamforming algorithm for ESPAR antennas," *IEEE Antennas Wireless Propag. Lett.*, vol. 7, pp. 745–748, 2008.
- [7] O. N. Alrabadi, C. Divarathne, P. Tragas, A. Kalis, N. Marchetti, C. B. Papadimas, and R. Prasad, "Spatial multiplexing with a single radio: proof-of-concept experiments in an indoor environment with a 2.6-GHz prototype," *IEEE Commun. Lett.*, vol. 15, no. 2, pp. 178–180, 2011.
- [8] A. Kalis, A. Kanatas, and C. B. Papadimas, *Parasitic Antenna Arrays for Wireless MIMO Systems*. Springer, 2014.
- [9] B. Han, V. Barousis, C. Papadimas, A. Kalis, and R. Prasad, "MIMO over ESPAR with 16-QAM modulation," *IEEE Wireless Commun. Lett.*, vol. PP, no. 99, pp. 1–4, 2013.
- [10] D. V. Thiel and S. Smith, *Switched Parasitic Antennas for Cellular Communications*. Artech House, 2002.
- [11] A. Suarez, *Analysis and Design of Autonomous Microwave Circuits*. Wiley-IEEE Press, 2009.
- [12] S. Alamouti, "A simple transmit diversity technique for wireless communications," *IEEE J. Sel. Areas Commun.*, vol. 16, no. 8, pp. 1451–1458, 1998.
- [13] C. Bowick, C. Ajluni, and B. Blyler, *RF Circuit Design*, 2nd ed. Newnes, Elsevier, 2007.
- [14] K. L. Buon, J. B. Andersen, G. Kristensson, and A. F. Molisch, "Impact of matching network on bandwidth of compact antenna arrays," *IEEE Trans. Antennas Propag.*, vol. 54, no. 11, pp. 3225–3238, 2006.
- [15] C. G. Kakoyiannis and P. Constantinou, "Compact printed arrays with embedded coupling mitigation for energy-efficient wireless sensor networking," *International J. Antennas Propag.*, 2010.